

Resonant Tunneling in Truly Axial Symmetry Mn_{12} Single-Molecule Magnets: Sharp Crossover between Thermally Assisted and Pure Quantum Tunneling

W. Wernsdorfer¹, M. Murugesu², and G. Christou²

¹Lab. L. Néel, associé à l'UJF, CNRS, BP 166, 38042 Grenoble Cedex 9, France

²Dept. of Chemistry, Univ. of Florida, Gainesville, Florida 32611-7200, USA

(Dated: March 21, 2021)

Magnetization measurements of a truly axial symmetry Mn_{12} -*t*BuAc molecular nanomagnet with a spin ground state of $S = 10$ show resonance tunneling. This compound has the same magnetic anisotropy as Mn_{12} -Ac but the molecules are better isolated and the crystals have less disorder and a higher symmetry. Hysteresis loop measurements at several temperatures reveal a well-resolved step fine-structure which is due to level crossings of excited states. All step positions can be modeled by a simple spin Hamiltonian. The crossover between thermally assisted and pure quantum tunneling can be investigated with unprecedented detail.

PACS numbers: 75.50.Xx, 75.60.Jk, 75.75.+a, 75.45.+j

$[\text{Mn}_{12}\text{O}_{12}(\text{O}_2\text{CCH}_3)_{16}(\text{H}_2\text{O})_4] \cdot 2\text{CH}_3\text{CO}_2\text{H} \cdot 4\text{H}_2\text{O}$, Mn_{12} -Ac for short, was the first single-molecule magnet (SMM), exhibiting slow magnetization relaxation of its $S = 10$ spin ground state which is split by axial zero-field splitting [1]. It was also the first system to show thermally assisted tunneling of magnetization [2, 3, 4]. During the last several years, many more SMMs have been discovered and they are now among the most promising candidates for observing the limits between classical and quantum physics since they have a well defined structure, spin ground state and magnetic anisotropy [5, 6, 7, 9]. Nevertheless, Mn_{12} -Ac is still the most widely studied SMM [10, 11, 12, 13, 14, 15, 16, 17, 18, 19, 20, 21, 22]. While a rough understanding of the quantum phenomena in Mn_{12} -Ac was clear from the early studies, a detailed understanding has not yet emerged. For example, current theoretical models assume the presence of quadratic and quartic transverse crystal-field interactions in the spin Hamiltonian, where the former has been ascribed to solvent disorder [21]. However, these interactions, which contain only even powers of the raising and lowering operators, do not provide an explanation for the observation of odd tunneling steps in the hysteresis loops. It has been proposed that easy-axis tilting might give the missing odd transverse interactions [18]. Although such solvent disorder induced tilts exist, the tilt values are still unclear [24]. Hyperfine, dipolar, and Dzyaloshinsky-Moriya interactions were also proposed to be responsible for odd transverse terms [10, 13].

Other theoretical and experimental studies concern the crossover between thermally assisted and pure quantum tunneling [11, 12, 13, 14, 15, 22, 23]. The crossover can occur in a narrow temperature interval with the field at which the system crosses the anisotropy barrier shifting abruptly with temperature, or the crossover can occur in a broad interval of temperature with this field changing smoothly [15, 22, 23]. The first studies were published on Mn_{12} -Ac [11, 12, 13] but significant distributions of mol-

ecular environments are unfortunately present, and these complicate the interpretation of the data [14, 21].

We present here resonant quantum tunneling measurements of a recently discovered analog of Mn_{12} -Ac, namely $[\text{Mn}_{12}\text{O}_{12}(\text{O}_2\text{CCH}_2\text{Bu}^t)_{16}(\text{CH}_3\text{OH})_4] \cdot \text{CH}_3\text{OH}$, called Mn_{12} -*t*BuAc henceforth. We show that this compound has the same magnetic anisotropy as Mn_{12} -Ac but the molecules are better isolated and the crystals contain less disorder and a higher symmetry. Hysteresis loop measurements at several temperatures reveal a fine structure of steps which is due to the dominating energy level crossings. All step positions can be modeled by a simple spin Hamiltonian. The crossover between thermally assisted and pure quantum tunneling is investigated.

$[\text{Mn}_{12}\text{O}_{12}(\text{O}_2\text{CCH}_2\text{Bu}^t)_{16}(\text{H}_2\text{O})_4]$ was prepared by the carboxylate substitution procedure described elsewhere [25], and crystallizes in triclinic space group $P\bar{1}$ [26]. However, recrystallization from mixed $\text{CH}_3\text{OH}/\text{Et}_2\text{O}$ solvent gave Mn_{12} -*t*BuAc in tetragonal space group $I\bar{4}$. Full details of the synthesis, crystal structure and magnetic characterization are presented elsewhere [27]; the ground state spin $S = 10$ was established by magnetization measurements in the 1 - 7 T and 1.8 - 4.0 K ranges. The molecular structure of Mn_{12} -*t*BuAc is very similar to that of Mn_{12} -Ac except that the acetate (Ac) and H_2O groups have been replaced by $\text{Bu}^t\text{CH}_2\text{CO}_2$ (*t*BuAc) and CH_3OH groups, respectively. The increased bulk of the $\text{Bu}^t\text{CH}_2\text{CO}_2$ groups leads to a unit cell volume for Mn_{12} -*t*BuAc (7.06 nm^3) that is almost double that of Mn_{12} -Ac (3.72 nm^3), and thus to greater intermolecular separations and decreased intermolecular interactions relative to Mn_{12} -Ac. In addition, the interstitial CH_3OH solvent molecules in Mn_{12} -*t*BuAc are not disordered and neither are they hydrogen-bonding with the Mn_{12} molecules. As a result, the site symmetry of the latter in Mn_{12} -*t*BuAc is truly axial with a small distribution of environments. This is in stark contrast to Mn_{12} -Ac where each of the acetic acid ($\text{CH}_3\text{CO}_2\text{H}$) molecules in the crystal forms

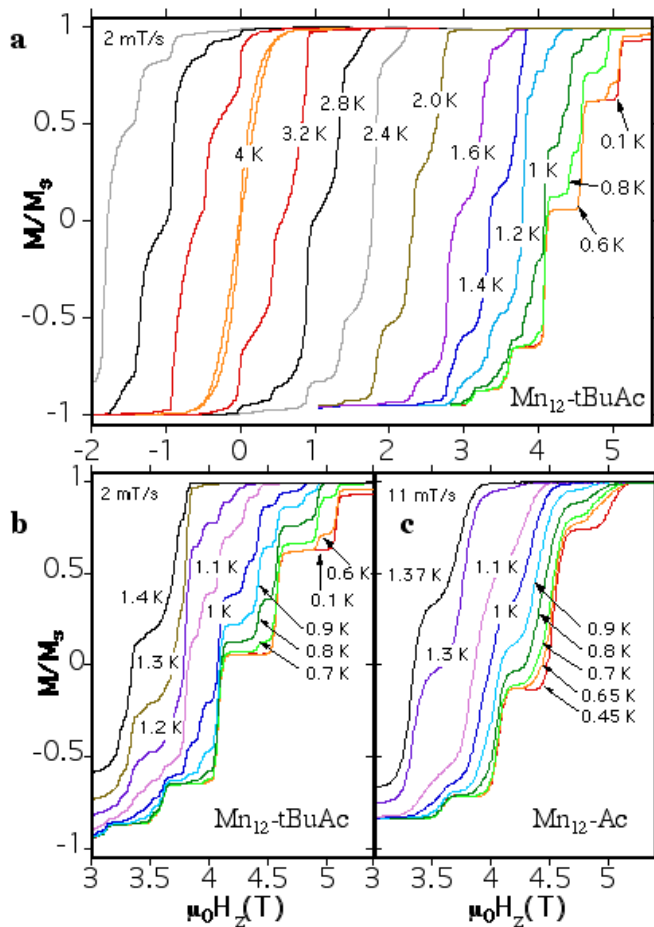


FIG. 1: (color online) Hysteresis loops of single crystals of (a-b) Mn_{12} -*t*BuAc and (c) Mn_{12} -Ac molecular clusters at different temperatures and a constant field sweep rate indicated in the figure. The data in (c) were taken from [13]. The loops display a series of steps, separated by plateaus. As the temperature is lowered, there is a decrease in the transition rate due to reduced thermal assisted tunneling. The hysteresis loops become temperature independent below 0.6 K, demonstrating quantum tunneling at the lowest energy levels.

a strong $\text{OH} \cdots \text{H}$ hydrogen-bond with a Mn_{12} molecule but will do so with only one of the two Mn_{12} molecules next to it. Since each Mn_{12} molecule is surrounded by four $\text{CH}_3\text{CO}_2\text{H}$ molecules, this disorder in the acetic acid orientation leads to the Mn_{12} molecules in Mn_{12} -Ac being hydrogen-bonded with k $\text{CH}_3\text{CO}_2\text{H}$ molecules ($k = 0 - 4$), with the $k = 2$ situation also having two possibilities (the two $\text{CH}_3\text{CO}_2\text{H}$ attached *cis* (adjacent) or *trans* (opposite) about the Mn_{12} molecule). Thus, although the Mn_{12} -Ac crystal possesses a crystallographic average symmetry of $I\bar{4}$, it contains a mixture of Mn_{12} molecules in six different hydrogen-bonded forms [21], and only two of these forms possess axial S_4 site symmetry, the $k = 0$ and 4 forms. The other forms have lower (rhombic) symmetry. As a result, Mn_{12} -Ac crystals contain Mn_{12} molecules with a wide distribution of

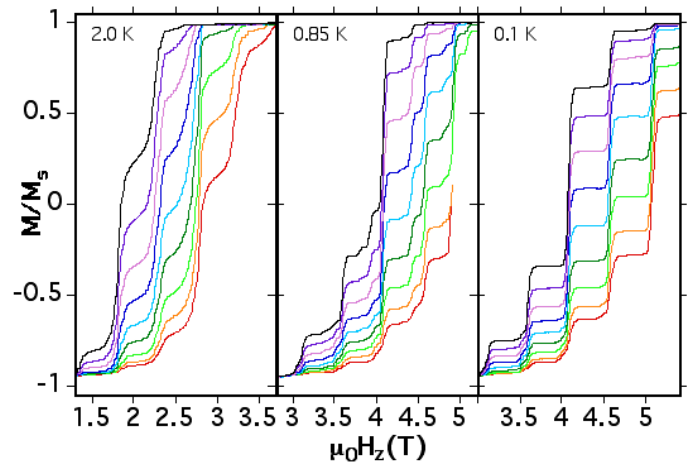


FIG. 2: (color online) Hysteresis loops of single crystals of Mn_{12} -*t*BuAc at several field sweep rates and at 2, 0.85 and 0.1 K. The field sweep rates from top to bottom are 0.2, 0.5, 1, 2, 4, 8, 17, 35, and 70 mT/s.

environments. Consequently, crystals of Mn_{12} -*t*BuAc are concluded to be far superior to those of Mn_{12} -Ac for detailed studies such as those in this paper, and this has indeed turned out to be the case. Finally, the axes of the tetragonal site symmetry of each molecule coincide with those of the unit cell, which is not the case for Mn_{12} -Ac

The magnetization measurements were performed by using a magnetometer consisting of several $6 \times 6 \mu\text{m}^2$ Hall-bars [28] on top of which a single crystal of Mn_{12} -*t*BuAc was placed. The field can be applied in any direction by separately driving three orthogonal superconducting coils. The field was aligned with the easy axis of magnetization using the transverse field method [24]. The applied field H_z was corrected because the determination of the resonance fields must take into account the internal magnetic field [29]. The sample dimensions were about $20 \times 15 \times 10 \mu\text{m}$. The Hall bars were patterned by Thales Research and Technology in Orsay, using photolithography and dry etching, in a delta-doped AlGaAs/InGaAs/GaAs pseudomorphic heterostructure grown by Picogiga International.

Fig. 1 shows the temperature dependence of the hysteresis loops of Mn_{12} -*t*BuAc and Mn_{12} -Ac SMMs. The loops display a series of steps, separated by plateaus. As the temperature is lowered, the hysteresis increases because there is a decrease in the transition rate of thermal assisted tunneling [3, 4]. The hysteresis loops become temperature independent below 0.6 K, demonstrating quantum tunneling at the lowest energy levels [11, 12, 13]. It is important to note that the loops remain strongly sweep rate dependent below 0.6K (Fig. 2). Apart from the major steps, these hysteresis loops reveal fine structure in the thermally activated regime which is also strongly sweep rate dependent (Fig. 2). This fine structure was first observed for Mn_{12} -Ac [11, 12, 13], see Fig. 1c, but it

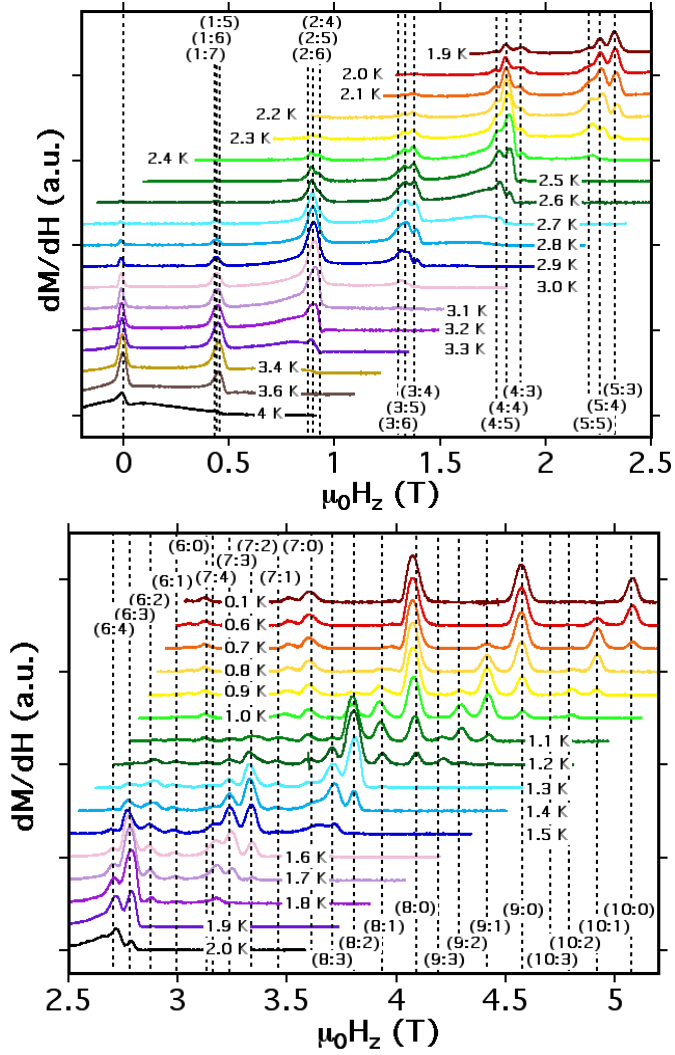


FIG. 3: (color online) Field derivative of the hysteresis loops of single crystals of $\text{Mn}_{12}\text{-}t\text{BuAc}$ at different temperatures. The applied field was swept from -6 T to 6 T at a constant field sweep rate of 2 mT/s. Resonant quantum tunneling of magnetization occurs at the peaks of dM/dH . The corresponding level crossings are labeled with two indexes $(n:p)$. The peaks coming from the faster relaxing impurity phase are not labeled.

is much clearer for $\text{Mn}_{12}\text{-}t\text{BuAc}$ (Figs. 1a, 1b, and 2). A convenient way of determining the field positions of the steps is to plot the derivative of the magnetization with respect to the applied field (Fig. 3). The step positions, that is the maxima of the relaxation rate, are given by the peaks on the dM/dH plot.

The simplest model describing the low-temperature spin dynamics of $\text{Mn}_{12}\text{-}t\text{BuAc}$ has the following spin Hamiltonian

$$\mathcal{H} = -DS_z^2 - BS_z^4 - g_z\mu_B\mu_0 S_z H_z + \mathcal{H}_{\text{trans}} \quad (1)$$

where S_x , S_y , and S_z are the three components of the

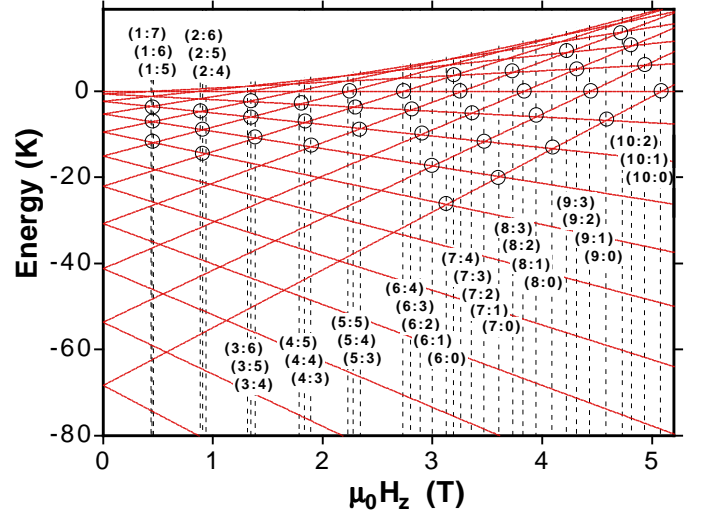


FIG. 4: (color online) Zeeman diagram of the 21 levels of the $S = 10$ manifold of Mn_{12} as a function of the field H_z applied along the easy axis. At $H_z = 0$, from bottom to top, the levels are labeled with quantum numbers $m = \pm 10, \pm 9, \dots, 0$. The resonant quantum tunneling steps which lead to a step height larger than $0.02 M_S$ at 2 mT/s occur at the indicated level crossings which are labeled with two indexes $(n:p)$.

spin operator, D and B are the anisotropy constants, the third term is the Zeeman energy associated with an applied field H_z , and the last term ($\mathcal{H}_{\text{trans}}$) describes small transverse terms containing S_x and S_y spin operators. Although $\mathcal{H}_{\text{trans}}$ produces tunneling, it can be neglected when determining the field positions of the level crossing because it is much smaller than the axial terms. Without $\mathcal{H}_{\text{trans}}$, the Hamiltonian is diagonal and the field dependence of the energy levels can be calculated analytically (Fig. 4). The energy level spectrum with $(2S + 1) = 21$ values can be labeled by the quantum numbers $m = -10, -9, \dots, 10$. At $\vec{H} = 0$, the levels $m = \pm 10$ have the lowest energy. When a field H_z is applied, the energy levels with $m < 0$ increase, while those with $m > 0$ decrease (Fig. 4). Therefore, energy levels of positive and negative quantum numbers cross at certain fields. The field position of the crossing of level $m = -S + p$ with $m' = S - n - p$ is given by

$$H_{(n:p)} = \frac{n [D + B ((-S + p)^2 + (S - n - p)^2)]}{g_z \mu_B \mu_0} \quad (2)$$

where $n = -(m + m')$ is the step index and $p = S + m$ labels the excited states ($p = 0$ for the ground state, $p = 1$ for the first excited state, etc.).

The step positions $H_{(n:p)}$, determined from Fig. 3, are shown in Fig. 5 [30]. The horizontal lines indicate the calculated energy level crossing fields using Eq. 2 with $D = 0.563$ K, $B = 1.2$ mK, and $g_z = 2$ where the latter was measured by EPR [18]. These values are very

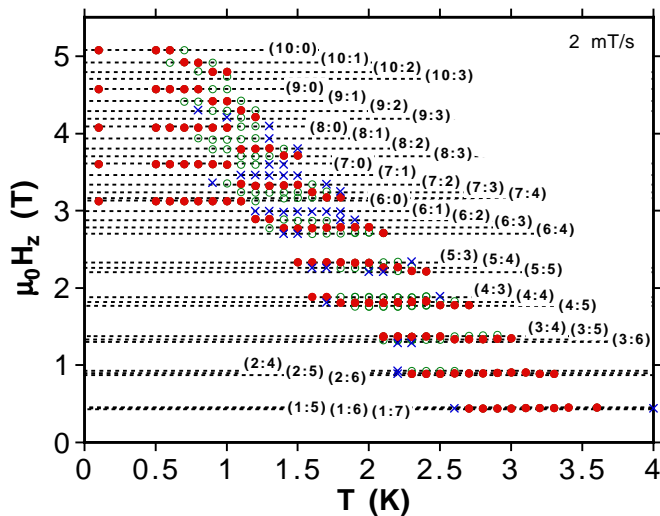


FIG. 5: (color online) Temperature dependence of the peak positions of dM/dH in fig. 3 at 2 mT/s. The horizontal lines indicate the calculated energy level crossing fields. The largest step for each n are filled dots whereas the others are open dots or crosses for step heights larger or smaller than $0.03 M_S$, respectively.

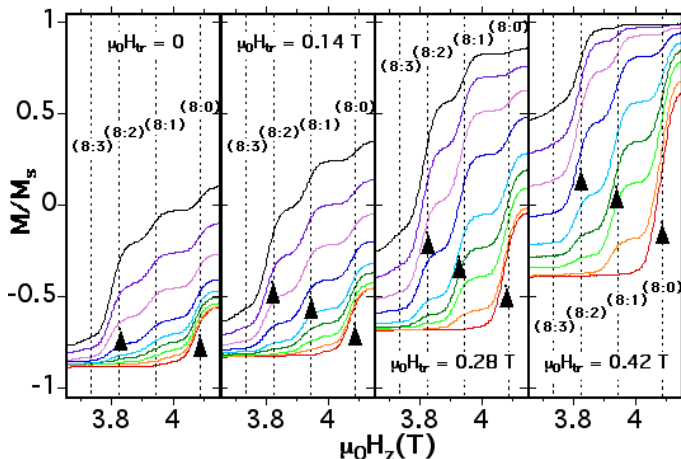


FIG. 6: (color online) Details of hysteresis loops at step $n = 8$ measured in the presence of four transverse fields H_{tr} and at temperatures of 0.1, 0.8, 0.9, 0.95, 1.0, 1.05, 1.1, 1.15, and 1.2 K from bottom to top. The field was ramped from -6 T to 6 T at a rate of 17 mT/s. The dominating steps are indicated.

close to those of Mn_{12} -Ac establishing that the magnetic cores of both molecules are comparable. Because the resonance fields of all avoided level crossings are well resolved, Mn_{12} -*t*BuAc allows the study in unprecedented detail of the crossover between thermally assisted and pure quantum tunneling. The dominant field steps for each step index n are shown in Fig. 5 by filled circles. Whereas the crossover is gradual for $n = 9$ and 10, a clear step is seen for $n = 8$. Indeed, the quantum step for (8:1)

is for all temperatures smaller than either (8:0) or (8:2). Similar results are found for $n = 7$ and 6. For $n \leq 5$, the crossover goes directly from non-measurable steps to finite ones with $p \geq 3$. Note that this sharp transition has not been observed in Mn_{12} -Ac [11, 12, 13]. It has been predicted that a sharp crossover can be smoothed out by applying a transverse field [15]. This can indeed be observed in Mn_{12} -*t*BuAc. Fig. 6 shows that about 0.14 T sufficiently increases the tunnel rate to smooth out the transition. Similar results were found for $n < 8$.

In conclusion, resonance tunneling measurements on a new high symmetry Mn_{12} -*t*BuAc molecular nanomagnet show levels of detail not possible with Mn_{12} -Ac, as a result of the much less disorder and higher symmetry in the crystals of the former. This has permitted an unprecedented level of analysis of the data to be accomplished, resulting in information not attainable with Mn_{12} -Ac. The crossover between thermally assisted and pure quantum tunneling can be easily explored and is found to be abrupt or gradual depending on the magnitude and orientation of the applied field. Simulation of the data allows D and B to be directly obtained from the step fine structure for the first time.

- [1] R. Sessoli, H.-L. Tsai, A. R. Schake, S. Wang, J. B. Vincent, K. Foltg, D. Gatteschi, G. Christou, and D. N. Hendrickson, *J. Am. Chem. Soc.* **115**, 1804 (1993); R. Sessoli, D. Gatteschi, A. Caneschi, and M. A. Novak, *Nature* **365**, 141 (1993).
- [2] M.A. Novak and R. Sessoli, in *Quantum Tunneling of Magnetization-QTM'94*, Vol. 301 of *NATO ASI Series E: Applied Sciences*, edited by L. Gunther and B. Barbara (Kluwer Academic Publishers, London, 1995), pp. 171–188.
- [3] J. R. Friedman, M. P. Sarachik, J. Tejada, and R. Ziolo, *Phys. Rev. Lett.* **76**, 3830 (1996).
- [4] L. Thomas, F. Lioni, R. Ballou, D. Gatteschi, R. Sessoli, and B. Barbara, *Nature (London)* **383**, 145 (1996).
- [5] C. Sangregorio, T. Ohm, C. Paulsen, R. Sessoli, and D. Gatteschi, *Phys. Rev. Lett.* **78**, 4645 (1997).
- [6] S. M. J. Aubin, N. R. Dilley, M. B. Wemple, G. Christou, and D. N. Hendrickson, *J. Am. Chem. Soc.* **120**, 839 (1998).
- [7] A. Caneschi, D. Gatteschi, C. Sangregorio, R. Sessoli, L. Sorace, A. Cornia, M. A. Novak, C. Paulsen, and W. Wernsdorfer, *J. Magn. Magn. Mat.* **200**, 182 (1999).
- [8] D. J. Price, F. Lioni, R. Ballou, P.T. Wood, and A. K. Powell, *Phil. Trans. R. Soc. Lond. A* **357**, 3099 (1999).
- [9] J. Yoo, E. K. Brechin, A. Yamaguchi, M. Nakano, J. C. Huffman, A.L. Maniero, L.-C. Brunel, K. Awaga, H. Ishimoto, G. Christou, and D. N. Hendrickson, *Inorg. Chem.* **39**, 3615 (2000).
- [10] N.V. Prokof'ev and P.C.E. Stamp, *Phys. Rev. Lett.* **80**, 5794 (1998).
- [11] A.D. Kent, Y. Zhong, L. Bokacheva, D. Ruiz, D.N. Hendrickson, and M.P. Sarachik, *EuroPhys. Lett.* **49**, 521 (2000).

- [12] L. Bokacheva, A.D. Kent, and M.A. Walters, Phys. Rev. Lett. **85**, 4803 (2000).
- [13] I. Chiorescu, R. Giraud, A.G.M. Jansen, A. Caneschi, and B. Barbara, Phys. Rev. Lett. **85**, 4807 (2000).
- [14] K. M. Mertes, Y. Suzuki, M. P. Sarachik, Y. Paltiel, H. Shtrikman, E. Zeldov, E. Rumberger, D. N. Hendrickson, and G. Christou, Phys. Rev. Lett. **87**, 227205 (2001).
- [15] D. A. Garanin and E. M. Chudnovsky, Phys. Rev. B **65**, 094423 (2002).
- [16] M. Dressel, B. Gorshunov, K. Rajagopal, S. Vongtragool, and A. A. Mukhin, Phys. Rev. B **67**, 060405(R) (2003).
- [17] M. Bal, J. R. Friedman, K. Mertes, W. Chen, E. M. Rumberger, D. N. Hendrickson, N. Avraham, Y. Myasoedov, H. Shtrikman, and E. Zeldov, Phys. Rev. B **70**, 140403(R) (2004).
- [18] S. Takahashi, R. S. Edwards, J. M. North, S. Hill, and N. S. Dalal, Phys. Rev. B **70**, 94429 (2004).
- [19] K. Park, T. Baruah, N. Bernstein, and M. R. Pederson, Phys. Rev. B **69**, 144426 (2004).
- [20] F. Luis, V. González, A. Millán, and J. L. García-Palacios, Phys. Rev. Lett. **92**, 107201 (2004).
- [21] A. Cornia, R. Sessoli, L. Sorace, D. Gatteschi, A. L. Barra, and C. Daiguebonne, Phys. Rev. Lett. **89**, 257201 (2002).
- [22] E. M. Chudnovsky and D. A. Garanin, Phys. Rev. Lett. **79**, 4469 (1997); D. A. Garanin E. M. Chudnovsky, Phys. Rev. B **57**, 13639 (1998).
- [23] Gwang-Hee Kim, Phys. Rev. B **59**, 11847 (1999); H. J. W. Mller-Kirsten et al., Phys. Rev. B **60**, 6662 (1999).
- [24] W. Wernsdorfer, N. E. Chakov, and G. Christou, Phys. Rev. B **70**, 132413 (2004).
- [25] M. Soler, P. Artus, K. Folting, J. C. Huffman, D. N. Hendrickson and G. Christou, Inorg. Chem. **40**, 4902 (2001).
- [26] M. Soler, W. Wernsdorfer, Z. Sun, J. C. Huffman, D. N. Hendrickson, and G. Christou, Chem. Commun. 2672 (2003).
- [27] M. Murugesu et al., to be submitted (2005).
- [28] L. Sorace, W. Wernsdorfer, C. Thirion, A.-L. Barra, M. Pacchioni, D. Mailly, and B. Barbara, Phys. Rev. B **68**, 220407(R) (2003).
- [29] The field H_z seen by a spin is roughly the sum of the applied field H_{appl} and the demagnetization field of the crystal. The latter can be determined by sweeping the applied field back and forth over a resonance transition. We found a nearly linear dependence which yield the following field correction: $\mu_0 H_z = \mu_0 H_{\text{appl}} + 0.04 \text{ T } M/M_S$
- [30] The studied crystal contained about 5% of molecules which showed faster relaxation, similar to crystals of $\text{Mn}_{12}\text{-Ac}$. The corresponding field steps of the impurity phase were ignored.